Prediction of Laser-Induced Thermal Damage of Fiber Mat and Fiber MatUD Reinforced Polymers

C.T. Pan and H. Hocheng

(Submitted 17 December 1997; in revised form 23 May 1998)

Laser machining of composites offers several advantages over conventional methods, such as no tool wear and contact force-induced material disintegration. The drawback in using the laser is the formation of a heat affected zone (HAZ). In the current investigations, analytical heat conduction models are used to determine the extent of the HAZ for anisotropic materials. The conductivity models allow for consideration of the anisotropic heat conductivity for GlassMat/PP and GlassMatUD/PP. Extensive experiments were conducted on composite materials to examine HAZ. The predictions of the analysis are compared with experimental results. The analytical results show a good agreement with experiments. The objective of this study is to optimize the work process.

Keywords chopped fibers, composites, laser, thermally-induced damage

1. Introduction

Composite materials exhibit poor quality cut surfaces due to spalled fibers, fuzzing, and delamination when routed by conventional tools. Special arrangements and careful optimization of cutting parameters are required therefore to avoid material deterioration and tool wear. Laser beam cutting offers an ideal means for the cutting of fiber composite materials being a noncontact and virtually force-free manufacturing method. Hence, laser machining is the appropriate method for the cutting to size of semiproducts, as well as for the subsequent machining of the contours of components.

However, in the shaping operation of composite materials after curing, thermal damage associated with laser energy can be produced. It leads to poor assembly tolerance and long-term performance deterioration. In the current research, preliminary analytical and experimental analyses reveal that the laser energy per unit length determines mainly the induced thermal damage. Heat conduction is maximum along the fibers, and the heat affected zone (HAZ) shape is thus affected by the beam scanning direction relative to fiber orientation.

The study investigates the grooving of (UD) carbon/epoxy as well as GlassMat20UD20(Strupp and Wenckler, Germany)/polypropylene (PP), demonstrating clearly thermal damage in 90° (i.e., perpendicular grooving) and 0° (i.e., parallel grooving) relative to the fiber axis. To simplify the heat conduction model, all experiments conducted in this study were grooving the workpiece instead of cutting through the workpiece. Conversely, GlassMat/PP was assumed to be semiisotropic and therefore independent of grooving direction.

A theoretical analysis based on moving point heat source was used to determine the extent of thermal damage in correlation with process parameters and material properties. Anisotropic heat conductivity models for thermal analysis are presented. Here, the extent of HAZ is estimated by the isotherm of the matrix char temperature. The mirror image method was used for specimen of finite thickness. Taking the immersing heat source into account would further improve the prediction of HAZ.

Besides, the absorbability of laser beam is good for most composites. Thus, the potential of laser cutting for composite materials is worth exploring. The related research is however limited and focused on machinability tests. Tagliaferri (Ref 1) conducted an experimental study to determine the surface finish characteristics of carbon fiber-reinforced plastics (CFRP) and aramide fiber-reinforced plastics (AFRP) by CO_2 laser. The HAZ depends strictly on feed rate. The higher the speed of laser beam, the smaller the volume of damage and the better the cut finish. Graphite-reinforced composites were found to be less suitable for laser cutting due to high fiber conductivity and vaporization temperature (Ref 1, 2). Caprino and Tagliaferri (Ref 2) developed a simple one-parameter thermal model, predicting the maximum feed rate as a function of beam power. An analysis of groove depth and width was conducted for composite materials. Good agreement was obtained between model predictions and experimental results (Ref 3, 4). Chryssolouris et al. (Ref 4) presented a concept of three dimensional machining. Threaded and turned workpieces can hereby be produced for carbon/teflon and glass/teflon materials.

2. Experiment

2.1 Experimental Setup and Materials

The laser beam (TEM_{00}) was supplied by two CO_2 laser with 1000 and 1500 W. Focused spots were 0.17 and 0.25 mm in diameter. Grooving experiments were conducted at beam power levels of 350 to 1500 W in continuous mode and at scanning velocities of 2.5 to 110 mm/s. A N_2 gas jet flow coaxial to the laser beam protects the focusing lens from debris and provides an inert environment for beam-material interaction.

To clearly illustrate the anisotropic characteristics of HAZ of fiber-reinforced plastics, material of test specimens was

C.T. Pan and **H. Hocheng,** Department of Power Mechanical Engineering, National Tsing Hua University, Hsinchu, Taiwan, R.O.C. Contact C.T. Pan at e-mail: d827717@oz.nthu.edu.tw.

laminated with UD prepreg laminates, carbon/epoxy, with fiber volume fractions of 50%. Carbon/epoxy is 8 mm in thickness (64 laminations) and 20 by 40 mm in area. The temperature of decomposition for the carbon/epoxy determined by thermal gravomatric analysis (TGA) is 360 °C (633 K), as shown in Fig. 1. The carbon/epoxy was prepared in a laboratory using the following process. The following steps, as shown in Fig. 2, produce test specimens: 1. Apply heating source upon laminates from room temperature to 123 °C for 60 min under 150 psi. 2. Continue to apply heating source from 123 to 183 °C for 120 min under 280 psi. 3. Cool laminates naturally from 185 °C to room temperature under 280 psi.

Other composite materials of GlassMat/PP and GlassMat-UD/PP used in this study were purchased from Strupp and Wenckler in Germany. GlassMat/PP is chopped glass fiber reinforced PP. Conversely, GlassMatUD/PP is chopped glass fiber reinforced PP, interlaminated by unidirectional glass fiber. In this study, series of GlassMat20/PP, GlassMat30/PP, GlassMat40/PP, GlassMat50/PP, and GlassMat20UD20/PP are tradenames owned by Strupp and Wenckler. Tables 1 and 2 describe information about the specimen.

Table 1 Specification of the investigated composite materials

Composite materials	Volume fraction, V_{fiber}/V_{matrix}, %	Thickness, D, mm	Fiber type
Carbon/epoxy	50/50	8	UD Fiber (HTS)
GlassMat20/PP	8/92	3.5	Chopped fiber
GlassMat30/PP	13/87	3.5	Chopped fiber
GlassMat40/PP	19/81	3.5	Chopped fiber
GlassMat50/PP	26/74	3.5	Chopped fiber
GlassMat20UD20/PP	21.2/78.8	3.7	Chopped and UD fiber

Unidirectional, UD

2.2 Experimental Procedure

Experimental parameters include the laser beam power, P, and grooving velocity, V. Experiments were performed to analyze HAZ, varying the process parameters, that is, laser beam power and traverse velocity. The relation between these parameters and HAZ will be discussed. Also, an energy density parameter (P/V) was used to incorporate all process conditions into one variable (Ref 5). This parameter relates the total amount of energy received in unit grooving length. In this study, it varies from 3 to 210 J/mm.

The width, W_d, of the HAZ is examined by optical microscope. W_d is the maximum width determined by the isotherm of $T = T_c$, where T_c is the matrix char temperature. The experimental results were then compared with the predictions.

3. Theoretical Analysis

3.1 Anisotropic Thermal Conductivity Models

In this research, thermal conductivity of the carbon/epoxy was measured by the laser flash method utilizing a Holometrix microflash instrument (Holometrix, Canada). This process conforms to ASTM E 146-92, "Standard Test Method for Thermal Conductivity of Solids by the Flash Method" for the measurement of thermal conductivity (Ref 6, 7). Table 2 lists the measured conductivities.

Table 2 Properties of the investigated composite materials

Composite materials	Volume fraction, V_{fiber}/V_{matrix}, %	Thermal conductivity, k_{fiber}/k_{matrix}, W/mK	Latent heat of vapor (fiber) L_v, kJ/kg	Composite conductivity k, W/mK
GlassMat20/PP	8/92	0.8/0.22	31000	$k_x = k_y = k_z = 0.241$
GlassMat30/PP	13/87	0.8/0.22	31000	$k_x = k_y = k_z = 0.255$
GlassMat40/PP	19/81	0.8/0.22	31000	$k_x = k_y = k_z = 0.273$
GlassMat50/PP	26/74	0.8/0.22	31000	$k_x = k_y = k_z = 0.296$
GlassMat20UD20/PP (90° grooving)	21.2/78.8	0.8/0.22	31000	$k_x = 0.243$ $k_y = 0.265$ $k_z = 0.243$
Carbon/epoxy (90° grooving)	50/50	8.5/0.35	41000	$k_x = 0.67$ $k_y = 4.50$ $k_{z = 0.67}$

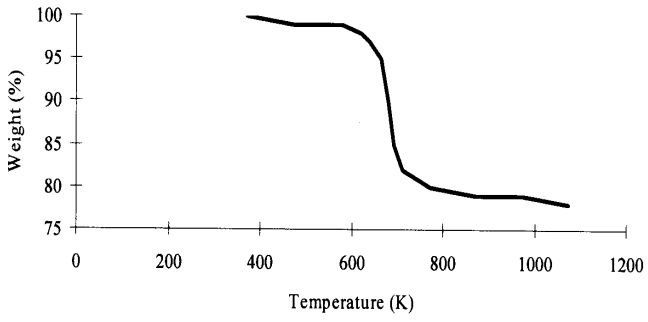

Fig. 1 Thermogravimetric analysis of carbon/epoxy

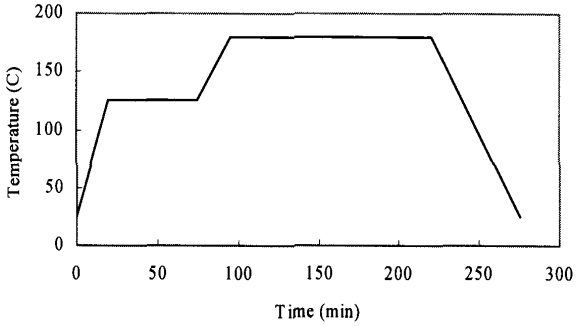

Fig. 2 Curing procedure of unidirectional carbon/epoxy

Chryssolouris et al. (Ref 3) presented a prediction model for the extent of HAZ based on isotropic heat conduction, and Springer and Tsai (Ref 8) defined an effective thermal conductivity for unidirectional laminates. The thermal conductivity parallel to the fiber direction is obtained by the rule of mixture (Ref 8), as shown in Fig. 3(a):

$$k_{parallel} = V_{fiber}k_{fiber} + V_{matrix}k_{matrix} \quad \text{(Eq 1)}$$

The existing micromechanical approach to predict the transverse thermal conductivity of unidirectional fiber reinforced plastics (FRP) from the properties of the constituents provides (Ref 8), as shown in Fig. 3(a):

$$k_{series} = \frac{k_{fiber}k_{matrix}}{V_{matrix}k_{fiber} + V_{fiber}k_{matrix}} \quad \text{(Eq 2)}$$

where V_{matrix} and k_{matrix} denote the volume fraction and the thermal conductivity of the matrix, whereas V_{fiber} and k_{fiber} stand for the corresponding properties of the fibers parallel to their longitudinal axis.

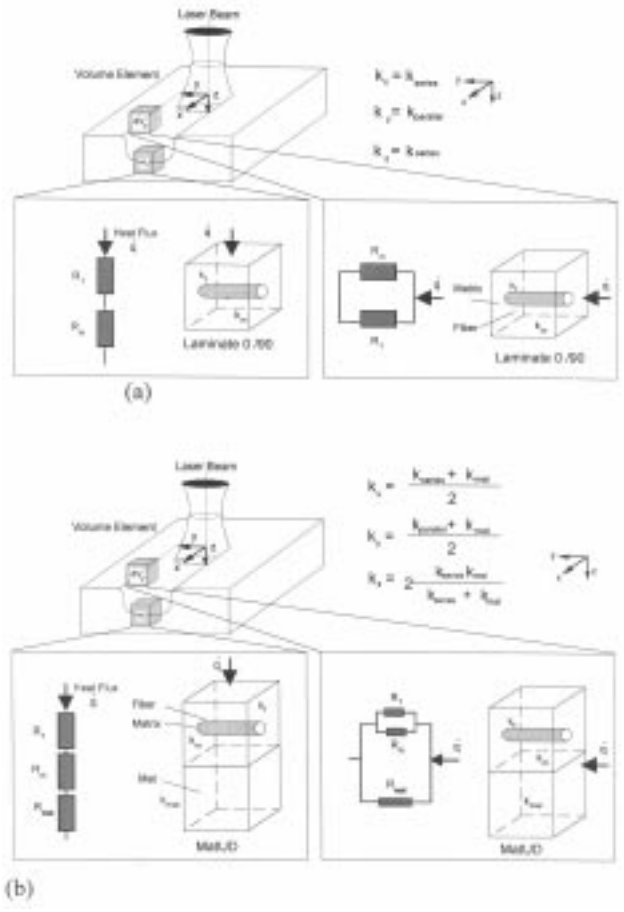

Fig. 3 Model of resistor. (a) Heat resistance of UD laminates (Ref 3, 8). (b) Heat resistance of GlassMat20UD20/PP (90 degree grooving)

In the case of GlassMat/PP, semiisotropic formation was assumed in the study. The formula (Ref 9) is adopted to evaluate the conductivity as shown in Eq. 3:

$$k_{mat} = k_{matrix}\frac{(1 - V_{fiber})k_{matrix} + (1 + V_{fiber})k_{fiber}}{(1 + V_{fiber})k_{matrix} + (1 - V_{fiber})k_{fiber}} \quad \text{(Eq 3)}$$

The measured thermal conductivities for UD carbon/epoxy, as listed in Table 2, can be precisely approached by Eq 1 and 2. Therefore, they are chosen in this study to provide further reasonable modifications to evaluate the conductivity of GlassMat20UD20/PP. In the case of grooving 90° relative to the fiber axis of GlassMat20UD20/PP, as far as the *y*-direction is concerned, both volume fractions are connected macroscopically in parallel. In the higher volume fraction, matrix and fiber are connected in parallel in contrast to the GlassMat/PP connected lower volume fraction, as shown in Fig. 3(b). Consequently, by coupling both cases:

$$k_x = \frac{k_{series} + k_{mat}}{2} \quad \text{(Eq 4)}$$

$$k_y = \frac{k_{parallel} + k_{mat}}{2} \quad \text{(Eq 5)}$$

and

$$k_z = 2\frac{k_{series}k_{mat}}{k_{series} + k_{mat}} \quad \text{(Eq 6)}$$

where k_x, k_y, and k_z are conductivities in *x*-, *y*-, and *z*-axis, respectively.

3.2 Heat Conduction Analysis

The study of anisotropic formation of HAZ in laser machining of fiber-reinforced plastics starts with a grooving along the principal material axes in unidirectional laminates. First, an anisotropic semiinfinite body subject to a point heat source moving along the *x*-axis at velocity, *V*, is analyzed. The erosion front is simplified, and the molten layer is assumed to have a negligible thickness (Ref 3). The principal axis heat conduction in the workpiece is governed by (Ref 10):

$$k_1\frac{\partial^2 T}{\partial x^2} + k_2\frac{\partial^2 T}{\partial y^2} + k_3\frac{\partial^2 T}{\partial z^2} = \rho c_p\frac{\partial T}{\partial t} \quad \text{(Eq 7)}$$

where k_1, k_2, and k_3 are principal conductivities.

To obtain the temperature field, the following assumptions were made:

- Three-dimensional heat conduction in the workpiece occurs normal to the erosion front, and the beam/material interaction results in complete material removal at the vaporization temperature.

- The thermal properties measured by laser flash method are independent of temperature. The secondary heat source from oxidation reaction is neglected because of inert surroundings.
- The evaporated material does not interfere with the laser beam, and multiple reflections of laser radiation within the groove are neglected.
- The energy used in the vaporization process is removed before significant heat conduction occurs.

For the current workpiece of a thin slab with thickness D, an analytical solution will be sought under the assumption of no heat conduction at the bottom surface, that is, $\partial T/\partial z = 0$ at $z = D$. However, the previously presented analytical model of infinite body with $\partial T/\partial z = 0$ at $z = \infty$ does not provide the desired boundary condition at $z = D$. Hence a modification is needed to satisfy the thin slab boundary condition. The mirror image method can be employed for this purpose (Ref 11). The calculated temperature field is

$$T - T_0 = -\Phi_0(x,y,z) + \sum_{n=0}^{\infty} [\Phi_n(x,y,z_n) + \Phi'_n(x,y,z'_n)] \quad \text{(Eq 8)}$$

where Φ is temperature field function:

$$z_n = 2nD - z \quad z'_n = 2nD + z \quad n = 0, 1, 2, 3 \quad \text{(Eq 9)}$$

In previous analysis, the location of the heat source is considered not at $z = 0$ as adopted. For accuracy and simplicity, the heat source is assumed to move at groove depth (z_0). Hence, the temperature field can be obtained as follows:

$$T - T_0 = \frac{\eta P e^{\frac{v\rho c_p x}{2k_1}}}{2\pi(k_1k_2k_3)^{1/2}} \left[\frac{e^{\frac{v\rho c_p(\gamma)}{2\sqrt{k_1}}}}{\gamma} + \sum_{n=1}^{\infty} \left(\frac{e^{-\frac{v\rho c_p(\gamma_{2n})}{2\sqrt{k_1}}}}{\gamma_{2n}} + \frac{e^{-\frac{v\rho c_p(\gamma_{2n+1})}{2\sqrt{k_1}}}}{\gamma_{2n+1}} \right) \right] \quad \text{(Eq 10)}$$

where

$$\gamma = \sqrt{\frac{x^2}{k_1} + \frac{y^2}{k_2} + \frac{(z - z_0)^2}{k_3}}$$

$$\gamma_{2n} = \sqrt{\frac{x^2}{k_1} + \frac{y^2}{k_2} + \frac{(2nD - (z - z_0))^2}{k_3}},$$

and

$$\gamma_{2n+1} = \sqrt{\frac{x^2}{k_1} + \frac{y^2}{k_2} + \frac{(2nD + (z - z_0))^2}{k_3}} \quad \text{(Eq 11)}$$

The extent of the HAZ is then determined by the isotherm of the matrix char temperature. Iterations between the groove depth and the extent of HAZ are carried out until the required convergence is reached.

4. Results and Discussions

The temperature of decomposition for carbon/epoxy was determined by TGA, as shown in Fig. 1. $T = T_c$ can be integrated into Eq 10. T_c = 633 K was taken in this simulation for epoxy, where 5wt% of epoxy decomposition is occurred (see Fig. 1), T_c = 438 K for PP, and T_c = 403 K for polyethylene (PE) (Ref 12). The extent of HAZ can be solved with Eq 10. The coefficient of laser absorption is assumed to be $\eta = 1$ (Ref 3).

As shown in Fig. 4, grooving perpendicular to fiber orientation of carbon/epoxy is more severely affected than grooving parallel to fiber orientation in the current experiment. This is explained by the fact that carbon fiber has a much higher thermal conductivity than epoxy. In the case of grooving parallel to

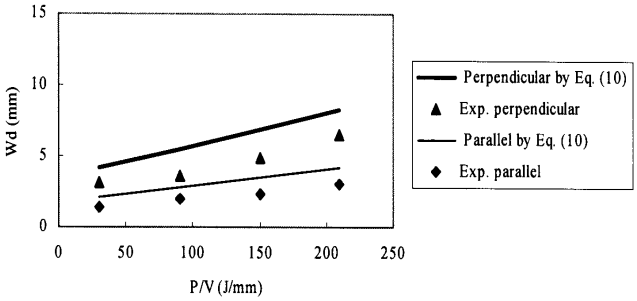

Fig. 4 Prediction of heat affected zone for carbon/epoxy as a function of the energy per unit length (Pr = 200 KPa)

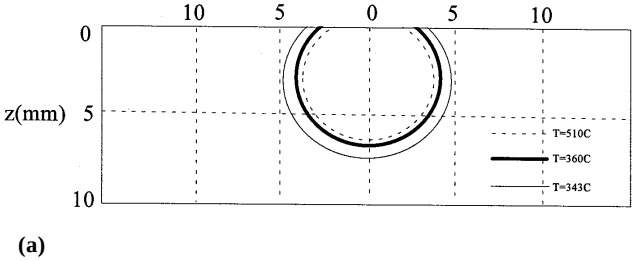

(a)

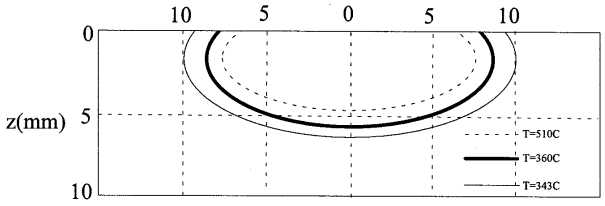

(b)

Fig. 5 Calculated extent of heat affected zone for unidirectional carbon/epoxy predicted by Eq 23 (P/V = 210 J/mm, Pr = 200 KPa). (a) Parallel grooving, fibers in x axis. (b) Perpendicular grooving, fibers in y-axis.

fiber axis, the thermal conduction occurs mainly along the fiber direction. Consequently, the thermal effect is dammed across the fibers and limited to a narrow zone. Therefore, the resulting HAZ is less extensive in the parallel grooving case than in the perpendicular case.

Iterations for the extent of HAZ are conducted until a satisfactory convergence is reached. The extent of HAZ is then determined by the isotherm of the matrix char temperature considering a range char temperature. Figure 5 shows the calculated extent of HAZ.

The current tests and simulations show that HAZ is approximately proportional to the specific laser energy P/V (Fig. 4, 5). The HAZ seems to remain constant as long as the workpiece has to be grooved at a certain level of specific laser energy. The simulations of HAZ for grooving carbon/epoxy and GlassMat20/PP are compared with experimental results, as shown in Fig. 4 to 6.

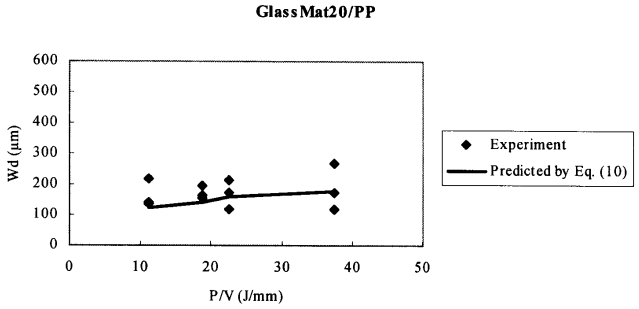

Fig. 6 Prediction of heat affected zone for GlassMat20/PP as a function of energy per unit length (Pr = 300 KPa)

The extent of HAZ as a function of *V* obtained by iterations of Eq 10, as well as by experimental results is shown in Fig. 7. It can be seen that HAZ is reduced by increasing the laser traverse velocity, that is, the larger the velocity, the smaller the thermal damage that will be produced.

Figure 8(a) shows the effects of various heat conductivities. It reveals that HAZ increases with *k*, that is, the higher the conductivity the larger the HAZ. Thus, in the case of grooving series of GlassMat/PP, grooving GlassMat50/PP produces the largest HAZ.

It is worth noticing that GlassMat/PP and GlassMatUD/PP are more suitable for laser machining than carbon/epoxy because of the smaller conductivities, as mentioned previously. The phenomena also can be seen in Table 2. GlassMat/PP and GlassMatUD/PP have smaller conductivities in their *y*-direction than carbon/epoxy. Thus, grooving carbon/epoxy produces larger HAZ than GlassMat/PP and GlassMatUD/PP.

The influence of power on HAZ can be analyzed using Eq 10. The effects of various power levels are shown in Fig. 8(b). It reveals that HAZ increases with *P*, that is, the higher the power the larger the HAZ.

5. Conclusions

An analysis for the extent of the HAZ in laser grooving of UD, Mat, and MatUD based on three-dimensional anisotropic

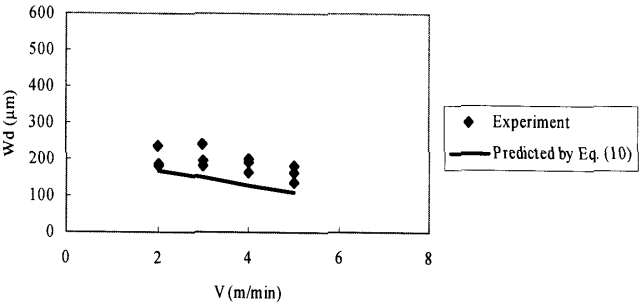

(a)

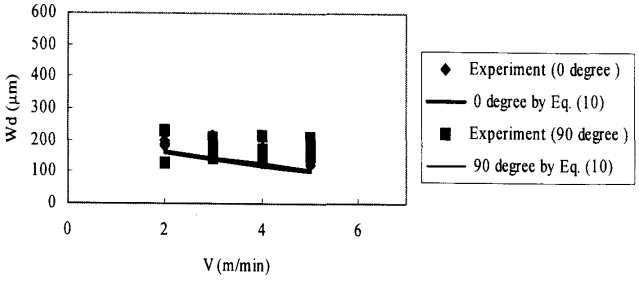

(b)

Fig. 7 Prediction of heat affected zone for GlassMat/PP and GlassMatUD/PP as a function of velocity (Pr = 300 KPa, P = 1250 W). (a) GlassMat30/PP. (b) GlassMat20UD20/PP

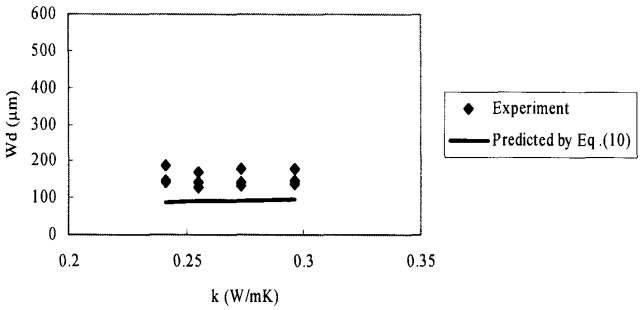

(a)

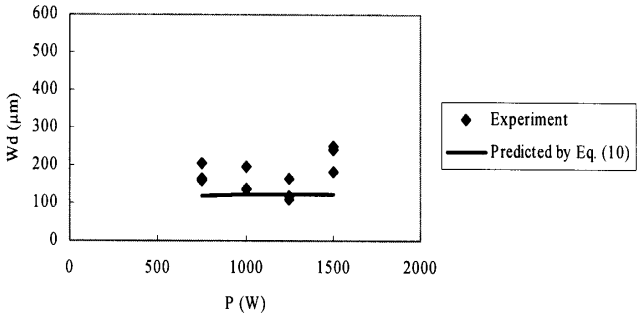

(b)

Fig. 8 Prediction of heat affected zone for GlassMat/PP as a function of conductivity and power (Pr = 300 KPa, P = 1250 W). (a) GlassMat20, 30, 40, and 50 /PP. (b) GlassMat30/PP

heat conduction and moving point heat source has been established. The analytical solutions include conductivity models for anisotropic composite materials. Thermal properties of composite materials for parallel and perpendicular grooving relative to fiber orientation were measured by the laser flash method and determined by the conductivity models for Glass-MatUD/PP. Modifications by the mirror image method were introduced to improve the prediction of the HAZ for workpieces of finite thickness. This study produced a good understanding of the various parameters that influence on the HAZ of laser grooving of composite materials. The developed models show good agreement with the experiments.

Acknowledgments

The authors wish to thank G. Spur and S. Liebelt, the Department of Machine Tools and Factory Management, TU Berlin, Germany, for support of the research. Also, the financial support from the National Science Council, Taiwan, on this project is appreciated.

References

1. V. Tagliaferri, A. DiIlio, and I.C. Visconti, Laser Cutting of FRP, *Composites,* Vol 16 (No. 4), 1985, p 317-325
2. G. Carprino and V. Tagliaferri, Maximum Cutting Speed in Laser Cutting of Fiber Reinforced Plastics, *Int. J. Mach. Tools Manuf.,* Vol 28 (No. 4), 1988, p 389-398
3. G. Chryssolouris, P. Sheng, and N. Anastasia, Laser Grooving of Composite Materials with the Aid of a Water Jet, *J. Eng. Ind. (Trans. ASME),* Vol 115, 1993, p 62-72
4. G. Chryssolouris, P. Sheng, and W.C. Choi, Three Dimensional Laser Machining of Composite Materials, *J. Eng. Mater. Technol. (Trans. ASME),* Vol 112, 1990, p 387-392
5. C.T. Pan and H. Hocheng, The Anisotropic Heat Affected Zone in the Laser Grooving of Fiber-Reinforced Composite Material, *J. Mater. Process. Technol.,* Vol 62, 1996, p 54-60
6. R.D. Cowan, Pulse Method of Measuring Thermal Diffusivity at High Temperature, *J. Appl. Phys.,* Vol 34, 1969, p 927-929
7. W.J. Parker, R.J. Jenkins, C.P. Butler, and G.L. Abbott, A Flash Method of Determining Thermal Diffusivity, Heat Capacity, and Thermal Conductivity, *J. Appl. Phys.,* Vol 32, 1961, p 679-684
8. G. Springer and S. Tsai, Thermal Conductivities of Unidirectional Materials, *J. Compos. Mater.,* Vol 1, 1967, p 166-173
9. A. Heber, "Modell zur rheologischen Auslegung faserverstärkter thermoplastischer Preßbauteile." *Dissertation Rheinland Westfalia Technological University,* Aachen, 1994
10. H.S. Carslaw and J.C. Jaeger, *Conduction of Heat in Solids,* Clarendon, London, 1959
11. T. Myint-U, *Partial Differential Equation of Mathematical Physics,* Elsevier North Holland, Inc., 1973
12. G. Spur and S. Liebelt, Modeling of Laser Cutting Composite and Comparison with Experiment, *Fourth Int. Conf. of Composites Engineering* (ICCE/4), Big Island, 1997, p 599-600